

Understanding cooperative behavior in structurally disordered populations

C. Xu¹, W. Zhang², P. Du¹, C.W. Choi³, and P.M. Hui^{3,a}

¹ College of Physics, Optoelectronics and Energy, Soochow University, Suzhou 215006, P.R. China

² Department of Electronics and Communication Engineering, Suzhou Institute of Industrial Technology, Suzhou 215104, P.R. China

³ Department of Physics, The Chinese University of Hong Kong, Shatin, New Territories, Hong Kong SAR, P.R. China

Received 17 October 2015 / Received in final form 10 April 2016

Published online 15 June 2016 – © EDP Sciences, Società Italiana di Fisica, Springer-Verlag 2016

Abstract. The effects of an inhomogeneous competing environment on the extent of cooperation are studied within the context of a site-diluted evolutionary snowdrift game on a square lattice, with the occupied sites representing the players, both numerically and analytically. The frequency of cooperation \mathcal{F}_C generally shows a non-monotonic dependence on the fraction of occupied sites ρ , for different values of the payoff parameter r . Slightly diluting a lattice leads to a lower cooperation for small and high values of r . For a range of r , however, dilution leads to an enhanced cooperation. An analytic treatment is developed for $\mathcal{F}_C = \mathcal{F}_C^l + \mathcal{F}_C^{ll}$, with \mathcal{F}_C^l emphasizing the importance of the small clusters of players especially for $\rho \ll 1$ and being treated exactly. A pair approximation for the contribution \mathcal{F}_C^{ll} from the other players is shown to be inadequate. A local configuration approximation (LCA) that treats the local competing configurations as the variables and amounts to include spatial correlation up to the neighborhood of a player's neighbors is developed. Results of $\mathcal{F}_C(\rho)$ and the number of different local configurations from LCA are in good agreement with simulation results. A transparent physical picture of the dynamics stemming from LCA is also presented. The theoretical approach provides a framework that can be readily applied to competing agent-based models in structurally ordered and disordered populations.

1 Introduction

How cooperative behavior could ever emerge in a population of selfish and competing individuals is an important question [1–9]. Different models that involve agents with competing strategies have been proposed and studied, with the aim of investigating the mechanism for the emergence of cooperation [7]. The prisoner's dilemma (PD) [1], for example, provides a paradigm with a Nash equilibrium corresponding to mutual defection. When PD is played repeatedly for an infinite number of rounds, however, cooperation could emerge [1,10]. In a population with spatial structure, agents are restricted to interact with a few connected neighbors. A simple structure is a two-dimensional (2D) square lattice in which a player is represented by a lattice point. It was found that cooperation could spread in such populations [3,11–14]. As a theoretical attempt, Nakamaru et al. [11] developed a mean-field approach and also the pair approximation which treats spatial correlation up to the neighbors, with results showing some of the main features as observed in simulation results. Besides regular lattices, how cooperation evolves in complex networks was also studied by simulations [15–17] and the

extent of cooperation was found to depend sensitively on the spatial structure. It is worthy to note that implementing the concept of co-action on symmetric games leads to cooperation as the rational outcome, even in one-shot games [18].

Disordered systems have been a topic of great interest [19]. Disorder plays an important role in systems in which the basic entities interact only when they are close to each other. Diluting a regular lattice randomly by taking away some sites, for example, leads to the percolation transition [20] that signifies a qualitative change in the connectivity in a system. Such dilution could also be coupled with other physics problems, e.g., the conductivity problem in random resistor networks [20] and critical phenomena associated with diluted Ising model [21]. In the context of competing games, Vainstein and Arenzon [22] studied a site-diluted model in which a fraction of randomly selected sites on a lattice are left empty and the remaining sites represent players. They found that cooperation is enhanced in disordered PD. Guan et al. studied the snowdrift game (SG) in the disordered lattice and found similar features [23]. Generally, a disordered lattice introduces an inhomogeneous competing environment as the number of nearest neighbors differs from player to player [24]. This is crucial when players adapt their action

^a e-mail: pmhui@phy.cuhk.edu.hk

by referencing to their neighbor's performance. Enhanced cooperation was also found for mobile players in disordered structures [23,25] when they engage in PD, SG [26], and Stag Hunt (SH) game [27]. A good understanding on the interplay between the extent of cooperation and spatial structures is essential and yet much remains to be explored. A good theoretical analysis on the effects of disordered lattices, for example, is lacking.

In the present work, we propose a site-diluted evolutionary snowdrift game and focus on studying the effects of disorder. Although there were similar simulation results reported [9,23] in disordered models using different evolutionary mechanisms, our focus is to present a theoretical framework that can be applied to a wide range of problems concerning competing games in disordered systems. This is a challenging task as theoretical analysis of evolutionary games in regular lattices is far from satisfactory, let alone disordered lattices. Hauert and Doebeli [26] developed a theory based on the pair-approximation for SG in regular lattices in which the players compare their average payoff for adapting their strategy in a synchronous manner. The theory could only capture the trend of how cooperation depends on the SG payoff parameter, but the key feature of the presence of a fully cooperative phase is missing. The pair approximation was shown to work better [28] when players update their strategies asynchronously after a round of the game with a chosen neighbor. Theories have also been developed recently for a few co-evolving systems in which an underlying dynamics drives changes in the network structure. These attempts include adaptive PD [29], dissatisfied adaptive SG [8,30], adaptive voter models [31–34], and co-evolving epidemics [35–38]. These theories typically aim at setting up dynamical equations [29,34,35,39] based on the evolutionary dynamics of the system. The number of variables and the number of equations increase with the range of spatial correlation that the theory aims to capture. General solutions are difficult to achieve [36] and often approximations are required to close the set of equations. Marceau et al. [40] proposed an improved compartmental method to account for the neighborhood of an agent in the adaptive epidemic model more precisely. The theory gives results in good agreement with simulation data [40,41]. When the compartmental method is applied to an evolving voter model [42,43], however, only qualitative agreement can be achieved [43]. It is important to consider the strength and the spatial extent of correlation in the dynamics in formulating a theory. For systems with weak correlation, mean-field theories based on a binomial closure scheme would suffice [8,44,45]. In lattices and diluted lattices in which the local competing environment is hardly randomized, it is expected that spatial correlation is too important to be ignored. The present work aims to shed light into the challenging question of formulating a theory for evolutionary games in a disordered competing environment.

The plan of the paper is as follows. In Section 2, we introduce the site-diluted evolutionary snowdrift game and present the key features of the model as obtained by numerical simulations. The extent of cooperation shows a

non-monotonic dependence on the fraction of diluted sites. In Section 3, we develop an analytic framework that separates the effects of the smaller clusters of players from that of the bigger clusters. The small clusters can be treated exactly. For the bigger clusters, we show that the pair approximation is inadequate. This inadequacy points to the necessity of incorporating a longer spatial correlation into the theory. A local configuration approximation (LCA) that includes the local competing environment of a player as well as the neighborhood of his opponents is introduced. In Section 4, results of LCA are shown to be in good agreement with simulation results. In a diluted lattice, LCA also gives a general and physically transparent picture of how players are continually re-distributed among possible payoff levels as the evolutionary dynamics proceeds. A summary is given in Section 5.

2 Site-diluted snowdrift game: model and key features

We propose and study a site-diluted snowdrift game on a square lattice. Consider a square lattice consisting of $\mathcal{N} = L \times L$ sites, with periodic boundary condition. In the site diluted case, a site is occupied by a player with a site-occupancy probability ρ . There are a total of $N = \rho\mathcal{N}$ players in the system. Players occupying two neighboring sites compete within the paradigm of a two-person evolutionary snowdrift game (SG). In SG, a player can take on one of two possible strategies or actions: to cooperate C or not-to-cooperate (to defect) D , with an action-updating scheme based on how well the current action performs. Within the context of a benefit b to both players when a task of a total cost c is completed, the payoff matrix of SG can be described by a single parameter r related to the cost-to-benefit ratio as [26]

$$\begin{array}{c} C \\ D \end{array} \left(\begin{array}{cc} C & D \\ 1 & 1-r \\ 1+r & 0 \end{array} \right) \quad (1)$$

with $0 < r < 1$, where the matrix elements give the payoffs to the player taking the action in the left-hand column, when playing against an opponent using the action in the top row.

At a moment in time, each player possesses an action. In the diluted SG, players have different numbers of opponents. The competing environment of the players becomes inhomogeneous. A local action-updating scheme that aims to achieve a better performance is implemented asynchronously as follows. We use capital letters to label players and lower-case letters to label actions. At each time step, a player I is chosen at random for a possible update of his action. The player I , who is taking action i ($i \in [C, D]$), competes with each of his k_I neighbors and gets an average payoff *per opponent* $V_{I,i}$ based on the actions of the opponents and according to the payoff matrix. Player I then randomly chooses a neighboring player J among his k_I neighbors as a reference player for an action update. Player J , who is taking action j ($j \in [C, D]$),

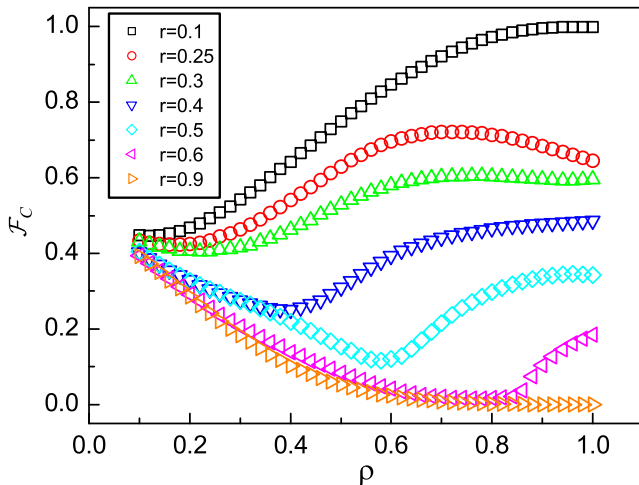


Fig. 1. The fraction of cooperative players or the frequency of cooperation $\mathcal{F}_C = N_C(\rho)/N$ as a function of the site-occupancy probability ρ on a diluted square lattice for different values of the payoff parameter r as obtained by numerical simulations.

competes with each of his k_J neighbors and gets an average payoff *per opponent* $V_{J,j}$. Player I then compares $V_{I,i}$ with $V_{J,j}$. If $V_{I,i} < V_{J,j}$, then player I will have a probability $w_{i \rightarrow j} = (V_{J,j} - V_{I,i})/\Omega$ to update his action from i to j of his better performing neighbor. Here, Ω is chosen to ensure $w_{i \rightarrow j} \leq 1$ and we take $\Omega = 1 + r$. If $V_{I,i} \geq V_{J,j}$, player I will keep his current action and thus $w_{i \rightarrow j} = 0$. Obviously, an isolated player will be using his initial action all the time.

To study the key features of the diluted SG, we have carried out numerical simulations on 100×100 lattices. We assume that a player is assigned an initial action randomly. For each value of the occupancy probability ρ and an initial configuration, the number of C -action players in the long-time steady state is obtained. Here, an initial configuration amounts to specifying a given configuration of occupied sites *and* an initial assignment of actions. For a given initial configuration, the action-updating scheme is carried out repeatedly in time (about 10^4 time steps) and the fraction of C -action players in the long-time limit (at least for 5×10^4 time steps) is determined. Results are then obtained by averaging over 100 different initial configurations. The averaged number of C -action players $N_C(\rho)$ for a given value of ρ can be shown in two ways. The ratio $\rho_C = N_C(\rho)/N$ gives the fraction of C -action players in the whole lattice, including the unoccupied sites. With a total of $N = \rho N$ players for a given ρ , it is more meaningful to focus on the reduced frequency of cooperation defined by the ratio $\mathcal{F}_C \equiv N_C(\rho)/N = \rho_C/\rho$ that gives the fraction of C -action players among all the players. It is also the probability that a randomly chosen player in the system taking on the C action. Figure 1 shows the dependence of \mathcal{F}_C on the occupancy probability ρ for different values of r that span the range $0 < r < 1$. The effects of r can be seen by noticing \mathcal{F}_C drops with an increasing r for a fixed value of ρ . This is in accordance with the meaning of the cost-to-benefit ratio r that cooperation

is suppressed when the cost to cooperate increases. For an evolutionary SG on a full square lattice ($\rho = 1$), there is an almost ALLC phase, i.e., all players are cooperative, at small r (e.g. see $r = 0.1$ results in Fig. 1) and an ALLD phase, i.e., all players are non-cooperative, at large r (e.g. see $r = 0.9$ results in Fig. 1) separated by a mixed phase at intermediate values of r [26]. The way that \mathcal{F}_C drops with r , however, depends on the value of ρ . This point is better illustrated by the dependence of \mathcal{F}_C on ρ as depicted in Figure 1. For a wide range of r , \mathcal{F}_C shows a non-monotonic dependence on ρ . When a full lattice is diluted, \mathcal{F}_C drops from its value at $\rho = 1$ for both $r \lesssim 0.2$ and $r > 0.3$. However, for $0.2 \lesssim r \lesssim 0.3$, diluting a full lattice would enhance cooperation and lead to a higher ρ_C/ρ . Further dilution (smaller ρ) leads to isolated clusters of players. For $\rho \approx 0$, only isolated individual players exist and $\mathcal{F}_C \approx 0.5$ due to the initial random assignment of actions. The results in Figure 1 show that \mathcal{F}_C drops from 0.5 with ρ for $\rho \ll 1$ for all values of r , and eventually turns around and increases with ρ for $r \leq 0.67$. These results show the intricate interplay between disorder and the cost-to-benefit ratio in determining the degree of cooperation. Although similar features were observed by simulations in previous studies on disordered PD [9,22] and SG [9,23], an analytic approach is lacking. Understanding this non-monotonic dependence of \mathcal{F}_C on the occupancy probability ρ is a challenging analytic task and the focus of the present work.

3 Theoretical analysis

Formulating a theory of \mathcal{F}_C in a full lattice is itself a non-trivial task. The pair approximation, for example, could at best capture the trend of \mathcal{F}_C as a function of r on a full lattice [26]. In diluted SG, the unoccupied sites create further complications and the non-monotonic dependence of \mathcal{F}_C on ρ turns out to be an excellent test bed for the validity of different analytic approaches, as we now discuss. A diluted SG consists of clusters of players of various sizes. Formally, the cooperation frequency is a combined result of the SG dynamics in a cluster of a certain size s and the distribution in cluster sizes. However, an approach of considering the dynamics of every possible cluster size will be too complicated and not too illuminating. Here, we aim at establishing an approximation that has the merits of being physically transparent and yet captures the key effects of site dilution for all values of ρ .

The key idea is to consider the effects of small clusters and big clusters separately. A line separating small and big clusters must then be drawn. To balance simplicity and accuracy, we simply treat the isolated players ($s = 1$) and isolated pairs of players ($s = 2$) as small clusters. Explicitly, we have

$$\begin{aligned} \mathcal{F}_C &= \sum_{\text{sizes } s} D(s) f_C^{(s)} = \sum_{s=1,2} D(s) f_C^{(s)} + \sum_{s>2} D(s) f_C^{(s)} \\ &\equiv \mathcal{F}_C^I + \mathcal{F}_C^{II}, \end{aligned} \quad (2)$$

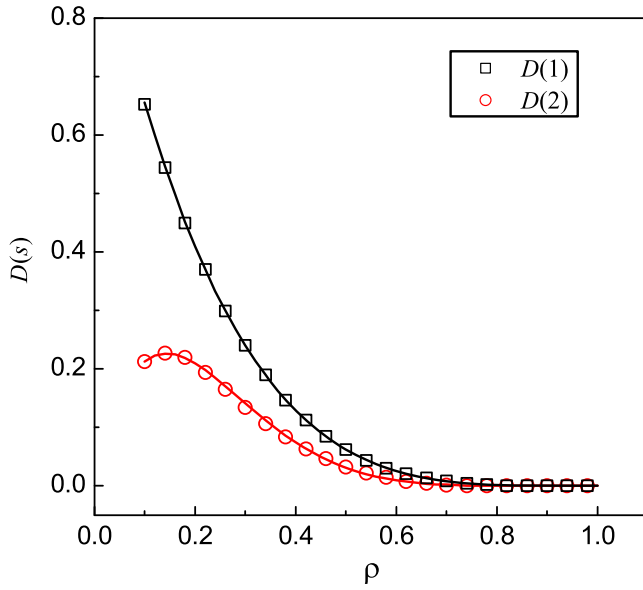


Fig. 2. The probabilities $D(1)$ (squares) and $D(2)$ (circles) of a randomly chosen occupied site belonging to an isolated site or an isolated pair of sites as obtained by numerical simulations. The lines are calculated by $D(1) = P(4, 0)$ and $D(2) = P(4, 1)P(3, 0)$ with $P(K, k)$ given by equation (3).

where $D(s)$ is the probability that a randomly chosen occupied site belonging to a cluster of size s and $f_C^{(s)}$ is the probability of finding a C -action player in a cluster of s players. The first summation is over all cluster sizes and the last equality defines the contributions from small (labelled I) and big (labelled II) clusters.

To handle the first term \mathcal{F}_C^I , we introduce $P(K, k)$ defined by

$$P(K, k) \equiv \binom{K}{k} \rho^k (1 - \rho)^{K-k}, \quad (3)$$

with $K = 4$ being the coordination number of a square lattice and $\binom{K}{k}$ the binomial coefficient. Physically, $P(K, k)$ is the probability that an occupied site has exactly k occupied sites among the K neighboring sites. In terms of $P(K, k)$, the probability of a randomly chosen player being an isolated player is $D(1) = P(K, 0)$. Similarly, the probability of a randomly chosen player belonging to an isolated pair of players is $D(2) = P(K, 1)P(K - 1, 0)$. A consistency check on the expressions of $D(1)$ and $D(2)$ is shown in Figure 2, in which both the analytic and simulation results are shown.

For the isolated players, half of them will take action C all the time as they will keep their initially assigned action and thus $f_C^{(1)} = 1/2$. For an isolated pair of players, the scenario is that of a cluster of two players in an evolutionary SG. Only when the initially assigned actions correspond to both players with action C , i.e., a C - C pair, the resulting actions will be C - C . All other initial assignments, i.e., C - D , D - C , and D - D , will evolve to a D - D pair as a result of the action updating mechanism.

Thus, $f_C^{(2)} = 1/4$. Putting the results together, we have

$$\mathcal{F}_C^I = \frac{1}{2} P(K, 0) + \frac{1}{4} P(K, 1)P(K - 1, 0). \quad (4)$$

Note that the dependence on ρ is embedded in $P(K, k)$. A few remarks follow, before we proceed to treat \mathcal{F}_C^{II} . The choice of treating clusters of sizes $s = 1$ and $s = 2$ separately is *necessary* because they dominate the behavior of \mathcal{F}_C for $\rho \ll 1$. However, their contributions drop as ρ increases. Carrying out a similar treatment for clusters of large sizes is complicated and turns out to be unnecessary. It is sufficient to treat the contributions of larger clusters in a continuum approximation, as we will show later.

3.1 Pair approximation for \mathcal{F}_C^{II} and its inadequacy

For players who are not isolated or not belonging to an isolated pair of players, we assume them to be in one big connected cluster and their contribution to \mathcal{F}_C is \mathcal{F}_C^{II} . Single-site approaches [46,47] will be too rough as the evolutionary SG involves pair-wise competitions. We therefore start our discussion with the pair approximation that focuses on the number of different types of links, namely C - C , C - D , D - C , and D - D , between neighboring players and examine its validity for treating \mathcal{F}_C^{II} . Summing up links of all types gives the total number of links \mathcal{L} . The variables are taken to be the link densities $f_{i,j}$, given by the number of (i, j) links divided by \mathcal{L} with (i, j) taking on (C, C) , (C, D) , (D, C) , and (D, D) . The sum rule $f_{C,C} + f_{C,D} + f_{D,C} + f_{D,D} = 1$ and the relation $f_{C,D} = f_{D,C}$ reduce the number of variables to two link densities. The frequency of cooperation in the cluster is then given by $f_C = f_{C,C} + f_{C,D}$ and \mathcal{F}_C^{II} follows. Here, \mathcal{F}_C within the pair approximation for \mathcal{F}_C^{II} is given by

$$\begin{aligned} \mathcal{F}_C &= \mathcal{F}_C^I + \mathcal{F}_C^{II} \\ &= \mathcal{F}_C^I + [1 - P(K, 0) - P(K, 1)P(K - 1, 0)]f_C, \end{aligned} \quad (5)$$

with \mathcal{F}_C^I given by equation (4). The value of f_C is calculated by equation (A.2) (see Appendix).

Figure 3 shows the theoretical results obtained by equation (5) together with the simulation results for four different values of r . The theory does *not* give results in agreement with simulation data. At best, it gives some qualitative features. For example, the pair approximation gives the increasing trend of \mathcal{F}_C with ρ for $r \ll 1$, as well as the non-monotonic behavior of \mathcal{F}_C with ρ for a wide range of larger r . Based on how the pair approximation [26,28,48–50] works in SG in regular lattices, we conclude that the pair approximation is inadequate in handling the disordered competing environments in the site-diluted SG. The failure also informs us that a better theory ought to include spatial information of the local competing environments more carefully.

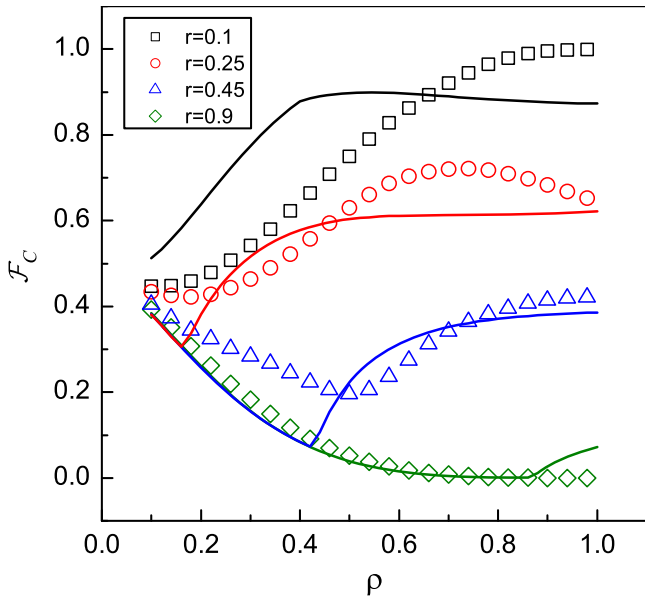


Fig. 3. The frequency of cooperation \mathcal{F}_C as a function of site-occupancy probability ρ for $r = 0.1, 0.25, 0.45,$ and 0.9 . The lines are calculated by the $\mathcal{F}_C = \mathcal{F}_C^I + \mathcal{F}_C^{II}$ with \mathcal{F}_C^I evaluated by the pair approximation. The symbols are results of numerical simulations. The pair approximation is inadequate for the full lattice and diluted lattices.

3.2 Local-configuration approximation for \mathcal{F}_C^{II}

We develop a local-configuration approximation (LCA) that focuses on how different local competing configurations change as the evolutionary dynamics proceeds. For a square lattice, the fundamental configuration of a player consists of a group of five sites – an occupied site together with its four surrounding sites that could be occupied or unoccupied. Figure 4 shows two examples of local configurations, with an occupied site in the middle with four occupied neighboring sites (Fig. 4a) and three occupied neighboring sites (Fig. 4b). Explicitly, let the occupied site at the center take on the action i ($i = C$ or D). The site and its immediate surrounding can be denoted by $i(j, l, m, n)$, where j, l, m, n could be C, D , or an empty site depending on the local configuration under consideration. The variables within LCA are then the frequencies of local configurations denoted by $f_i(j, l, m, n)$. The variables in local-configuration approximation, therefore, extends the spatial consideration from that of two neighboring sites in the pair approximation to that of a group of five sites.

To bring out the essence of LCA, we will focus on the case in Figure 4a and explain how dynamical equations can be established for such local configurations in detail. The fundamental configuration in Figure 4a consists of an occupied site I in the middle with the four occupied neighboring sites connected to the site I by the solid lines. For this class of configurations, the central site and its immediate surrounding is labelled by $i(j, l, m, n)$, where j, l, m, n could be C or D . As the evolutionary dynamics requires the comparison with the payoff of a neighboring player, the spatial extent for establishing the dynamical equations for

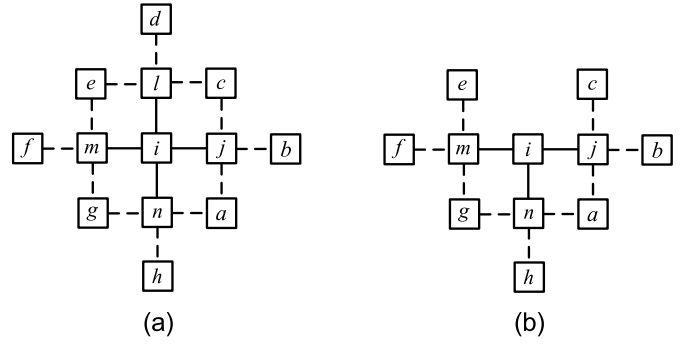


Fig. 4. Illustration of two local configurations with the central occupied site taking an action i ($i = C$ or D). (a) A local configuration consisting of the central site and four occupied nearest neighboring sites labelled by their actions j, l, m, n . The payoffs to these nearest neighboring sites are, in turn, determined by the sites that are two steps away from the central site as indicated by this cluster of sites around the central site. (b) A local configuration consisting of the central site and three occupied nearest neighboring sites. The payoffs to these sites are, in turn, determined by this cluster of sites around the central site.

$f_i(j, l, m, n)$ is actually farther than the nearest neighbors. To illustrate the point, if the neighboring player J using action j is chosen as a reference for an action update, his payoff is determined by the local configuration described by $j(b, c, i, a)$ as shown in Figure 4a, with the sites labelled by b, c and a being two steps (next-nearest) away from the central site and they can be an occupied site in the state of C or D , or unoccupied. Figure 4a shows the spatial extent that needs to be considered when the central site is chosen for an action update.

Dynamical equations for $f_i(j, l, m, n)$ can be set up following a similar consideration as in the pair approximation, despite being more complicated. First note that the probability of choosing a local configuration $i(j, l, m, n)$ for a possible action update is the frequency $f_i(j, l, m, n)$ itself. The neighboring sites of I are then considered in turn, say, starting from the site J on the right in an anti-clockwise way. Referring to Figure 4a, if the neighboring occupied site J is of action j , then we take the probability that $j(b, c, i, a)$ is its local configuration to be

$$p_j(b, c, i, a) = \frac{f_j(b, c, i, a)}{\sum_{b', c', a'} f_j(b', c', i, a')}, \quad (6)$$

where the summations in the denominator are over the possible states C, D , and empty for a', b', c' , i.e., over only three out of the four neighbors of j because the neighbor on the left (the central site) is under the condition of a given action i . The form of equation (6) amounts to assuming that every local configuration of the form $j(b', c', i, a')$ of an occupied site next to i appears with equal probability. Moving on to the site located above the central site i , if it is of action l , then we take the probability that

$l(c, d, e, i)$ is its local configuration to be

$$p_l(c, d, e, i) = \frac{f_l(c, d, e, i)}{\sum_{c', d', e'} f_l(c', d', e', i)}. \quad (7)$$

Similarly, for the site on the left of (below) the central site, if it is of action m (action n), then we take the probability that $m(i, e, f, g)$ ($n(a, i, g, h)$) is its local configuration to be

$$p_m(i, e, f, g) = \frac{f_m(i, e, f, g)}{\sum_{e', f', g'} f_m(i, e', f', g')}, \quad (8)$$

and

$$p_n(a, i, g, h) = \frac{f_n(a, i, g, h)}{\sum_{a', g', h'} f_n(a', i, g', h')}. \quad (9)$$

These quantities are useful in establishing the dynamical equations for the variables $f_i(j, l, m, n)$.

The probability of having an event that the central player of action i in a local configuration $i(j, l, m, n)$ adopts the action j of a neighboring player of local configuration $j(b, c, i, a)$ is given by the product of the probabilities that the referencing player is chosen among the neighbors and that the action update really takes place. The former is formally given by $1/k_i(j, l, m, n)$, where $k_i(j, l, m, n)$ is the degree or the number of neighboring occupied sites. For the case in Figure 4a, the probability is $1/4$. The latter is given by

$$w_{i \rightarrow j}(j, l, m, n) = \frac{V_{J,j}(b, c, i, a) - V_{I,i}(j, l, m, n)}{1 + r} \quad (10)$$

when the reference player is performing better, i.e., $V_{J,j}(b, c, i, a) > V_{I,i}(j, l, m, n)$. Otherwise, no action update will take place. When the action update is carried out, the number of the local configuration $i(j, l, m, n)$ drops by one and that of the local configuration $j(j, l, m, n)$ increases by one.

An important point in formulating the dynamical equations for the variables $f_i(j, l, m, n)$ is to incorporate the spatial correlation as manifested by the sharing of a common neighboring site (e.g. the one labelled c in Fig. 4a) by two nearest-neighboring sites (e.g. sites labelled j and l in Fig. 4a) of a local configuration. Starting from the site on the right of a local configuration, the possible local configurations $j(b, c, i, a)$ amount to allowing for all possible states of b' , c' and a' of the three neighboring sites out of four. For each of the local configurations $j(b, c, i, a)$, however, the local configurations $l(c, d', e', i)$ of the other nearest neighbor l correspond only to all possible states of d' and e' , i.e., two sites out of four. Similarly, for given $l(c, d, e, i)$, the local configurations for the site on the left $m(i, e, f', g')$ correspond only to all states of f' and g' . Finally, for given $j(b, c, i, a)$ and $m(i, e, f, g)$, the local configurations for the site below $n(a, i, g, h')$ correspond only to the possible states of h' . Finally, a set of dynamical equations for the frequencies of local configurations $i'(j', l', m', n')$ in the cases of Figure 4a can be formulated

by incorporating all the factors discussed. The equations are given by

$$\begin{aligned} \frac{df_{i'}(j', l', m', n')}{dt} = & \frac{1}{N} \sum_i \sum_{j, l, m, n} f_i(j, l, m, n) \\ & \times \sum_{b, c, a} p_j(b, c, i, a) \sum_{d, e} p_l(c, d, e, i) \\ & \times \sum_{f, g} p_m(i, e, f, g) \sum_h p_n(a, i, g, h) \\ & \times \sum_{z=j, l, m, n} \frac{w_{i \rightarrow z}(j, l, m, n)}{k_i(j, l, m, n)} \\ & \times [(\delta_{z, i'} - \delta_{i, i'}) \delta_{j, j'} \delta_{l, l'} \delta_{m, m'} \delta_{n, n'} \\ & + (\delta_{z, m'} - \delta_{i, m'}) \delta_{j, i'} \delta_{b, j'} \delta_{c, l'} \delta_{a, n'} \\ & + (\delta_{z, n'} - \delta_{i, n'}) \delta_{l, i'} \delta_{c, j'} \delta_{d, l'} \delta_{e, m'} \\ & + (\delta_{z, j'} - \delta_{i, j'}) \delta_{m, i'} \delta_{e, l'} \delta_{f, m'} \delta_{g, n'} \\ & + (\delta_{z, l'} - \delta_{i, l'}) \delta_{n, i'} \delta_{a, l'} \delta_{g, m'} \delta_{h, n'}], \quad (11) \end{aligned}$$

where the first and second summations are over the states of C and D for the indices i, j, l, m, n , and the other summations on the next-nearest neighbors of the central site are over the states of C, D , and empty sites. The delta functions in the parentheses account for the changes in the number of local configurations when an action update takes place.

Analysis on the change in the number of other local configurations can be carried out in a similar fashion. For the type of configurations as shown in Figure 4b, for example, we could again consider the neighboring sites of the central site one by one. When an empty neighboring site is encountered, we skip the site and move on to the next site. An empty site in the configuration affects the extent to which two neighboring sites of the central site share a common neighbor. Accounting for this effect leads to a set of dynamical equations for the local configurations shown in Figure 4b. Dynamical equations for other types of local configurations can also be formulated accordingly. Recall that the effects of isolated sites and isolated pair of sites are considered separately by \mathcal{F}^I .

A set of coupled dynamical equations for different local configurations $f_i(j, l, m, n)$ can be constructed within LCA. The equations are analogous to those (Eq. (A.2) in Appendix A) within the pair approximation, only that LCA includes a larger spatial correlation and thus consists of more variables. The equations can be iterated to the steady state to solve for $f_i(j, l, m, n)$. The frequency of cooperation in the cluster f_C , apart from the contributions of isolated sites and isolated pairs, is given by

$$f_C = \sum_{j, l, m, n} f_C(j, l, m, n), \quad (12)$$

where the summation is over all possible local configurations within LCA with the central site taking the action C . Finally, \mathcal{F}_C is again given by equation (5), with f_C calculated within LCA.

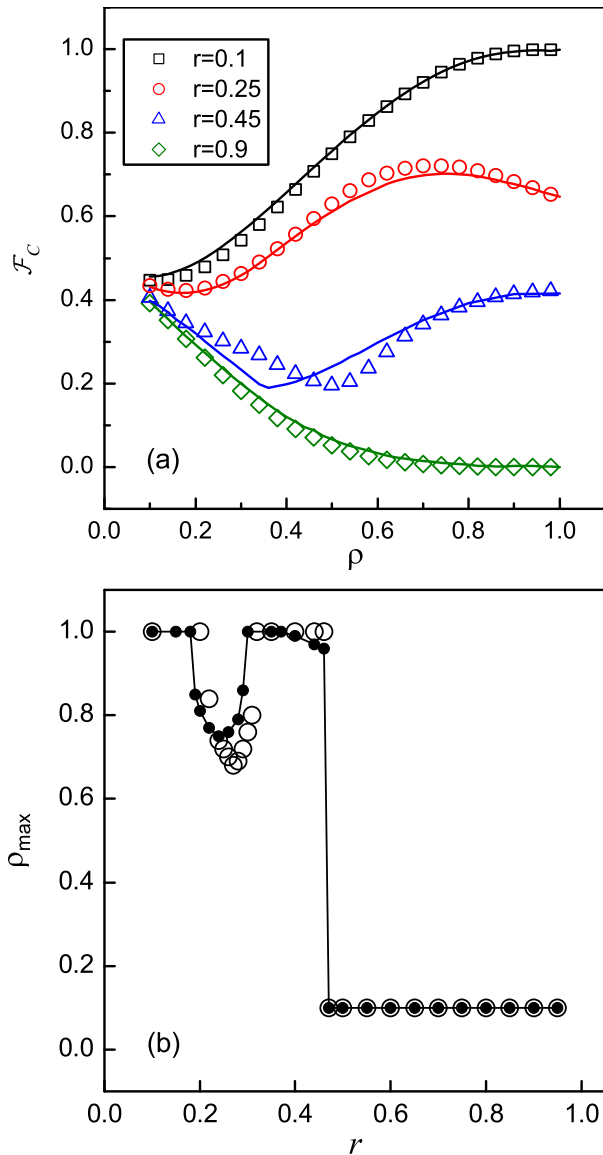


Fig. 5. (a) The frequency of cooperation \mathcal{F}_C as a function of the site-occupancy probability ρ as calculated by the local-configuration approximation (lines) and as obtained by numerical simulations (symbols) for different values of r . (b) For a given r , \mathcal{F}_C is highest at a certain occupancy probability $\rho_{max}(r)$. The dots (open circles) are obtained by numerical simulations (LCA).

4 Results of LCA and a physical picture

Results of \mathcal{F}_C as obtained by LCA are shown in Figure 5a for $r = 0.1, 0.25, 0.45$, and 0.9 , together with simulation results. The results capture the non-monotonic feature and they are in good agreement with simulation results. Comparing with results in Figure 3, the better performance of LCA over the pair approximation is evident. In particular, LCA gives the correct full-lattice (at $\rho = 1$) behavior, for which the pair approximation gives incorrect values of f_C with a large deviation at small r . For $r = 0.25$, LCA also correctly predicts an enhanced

cooperation when the lattice is slightly diluted and f_C attains a maximum at some optimal dilution. This feature is also missing within the pair approximation. At higher r (e.g. $r = 0.45$), maximum f_C is attained in a full lattice. Dilution from a full lattice leads to a drop in f_C until a minimum is reached. For large r (e.g. $r = 0.9$), cooperation is maximally suppressed in a full lattice and dilution serves to make cooperation possible by sustaining cooperation in small clusters such as isolated players and isolated pairs of players.

For each value of r , a highest frequency of cooperation occurs at some occupancy probability ρ_{max} that corresponds to where \mathcal{F}_C exhibits a maximum. Results of $\rho_{max}(r)$ as obtained by simulations (open circles) and by LCA (dots) are shown in Figure 5b. LCA captures the behavior of ρ_{max} very well.

Most noticeable in Figure 5 is the enhanced \mathcal{F}_C in the range $0.2 < r < 0.32$ when empty sites are introduced into an otherwise full lattice. In what follows, we give a qualitative and physically transparent explanation of this feature. Within this range of r , a maximum \mathcal{F}_C is attained at some optimal occupation with values $\rho > 0.6$, signifying that a spanning cluster exists in the system according to the percolation theory. Most of the occupied sites belong to this spanning cluster. The sites in the cluster could have different numbers of nearest neighbors given by $k = 1, 2, 3$, or 4 , unlike a full lattice where every site has the same number of nearest neighbors. For a player with k neighbors, there could be $n_C = 0, \dots, k$ neighbors using the C action. The payoff per opponent is then given by $V_C(k, n_C) = [n_C + (k - n_C)(1 - r)]/k$ for a player taking the C action, and $V_D(k, n_C) = n_C(1 + r)/k$ for a player taking the D action. For clarity, we introduced the symbol $V_C(k, n_C)$ ($V_D(k, n_C)$) to represent the payoff per opponent to a player of action C (action D) with exactly n_C neighbors of action C among his k neighbors. To illustrate the physical picture, we consider $r = 0.25$ within the range $0.2 < r < 0.32$ and show all the possible values of the payoffs per opponent $V_C(k, n_C)$ and $V_D(k, n_C)$ in Figure 6. There are $k + 1$ values of payoffs for a given k , with the highest payoff corresponding to $n_C = k$ and drops as n_C decreases. These discrete payoff levels for C -action (D -action) players are reminiscent of the energy levels in an energy band and thus we refer to the collection of payoff levels as the C -band (D -band) [51]. According to the action switching mechanism, players in the levels $V_C(k, k)$ and $V_D(k, 0)$ will not change their action, as all their neighbors are taking the same action. A D -action player surrounded only by C -action neighbors has the highest payoff per opponent of $V_D(k, k) = 1 + r$ and therefore the player will not take part in the action switching mechanism. The payoff levels of these three cases are marked as thinner lines in Figure 6.

Let us consider a full lattice of players, i.e., $\rho = 1$. In this case, only the $k = 4$ levels in the C -band and D -band are relevant. An initial condition of assigning an action randomly to every player amounts to distributing half of the players to the five levels in the C -band according to the binomial distribution, and the other half to the five levels

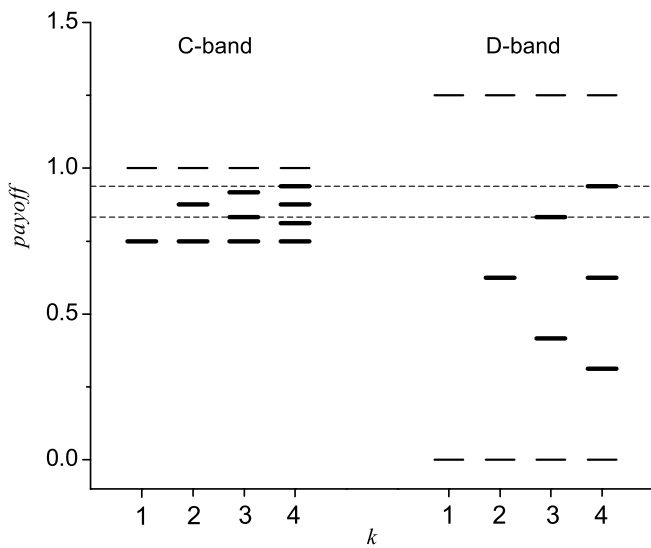


Fig. 6. Payoff levels $V_C(k, n_C)$ and $V_D(k, n_C)$ for $k = 1, 2, 3, 4$ and for $n_C = 0, \dots, k$ for a given k . The levels are evaluated for the case $r = 0.25$. The levels $V_C(k, n_C)$ and $V_D(k, n_C)$ collectively form the C -band and D -band, respectively. The levels illustrated by the thinner lines are those in which the central site in the configuration will not be affected by the action updating mechanism. Evolutionary dynamics amounts to a continual redistribution of players among these payoff levels.

in the D -band in a similar fashion. This initial distribution evolves in time in a restricted manner. Consider an action switching process of a C -action player, say, in the payoff level $V_C(4, n_C)$. The player will refer to one of his $4 - n_C$ neighboring D -action players. If there is a switching, the referencing D -action player must be one in a payoff level $V_D(4, n_C)$ that is higher than $V_C(4, n_C)$. The difference in payoffs drives an action switching that amounts to moving a player from $V_C(4, n_C)$ in the C -band to $V_D(4, n_C)$ in the D -band. Accompanying this change is a change in the local configuration of the four neighbors. These changes amount to moving players within the same band. In summary, the evolutionary dynamics can be interpreted as players making transitions between payoff levels crossing different bands and within the same band. The continual re-distribution of players among the payoff levels approaches a stationary distribution, analogous to that of a reaction approaching an equilibrium following the law of mass action. For a full lattice at $r = 0.25$, cooperation is generally promoted because $V_D(4, 1)$ and $V_D(4, 2)$ are both lower than all V_C payoffs. However, there exists a payoff level of $V_D(4, 3) = V_C(4, 3)$ that keeps a number of D -action players in the system. For smaller r , e.g. $r = 0.1$, $V_C(4, 3) > V_D(4, 3)$, and this is a reason why \mathcal{F}_C is higher at $r = 0.1$ than $r = 0.25$.

The effect of site dilution can also be clearly seen from the physical picture. Slightly diluting a lattice leads to a spanning cluster of occupied sites with different numbers of neighbors. The sites in a cluster could now have $k = 1, 2, 3$ or 4 . The effect is that all the payoff levels in Figure 6 can now be accessed by the players. As the unoccupied

sites are static, the number of neighbors for every player is fixed initially. This has the effect of restricting a player to stay in the payoff levels with the same k when making transitions across the bands and within the same band. As shown in Figure 6 for $r = 0.25$, site dilution introduces a number of payoff levels in the C -band and D -band, with those in the C -band generally higher in payoffs. In fact, only the levels $V_D(3, 2)$ and $V_D(4, 3)$ lie within the many levels in the C -band, as indicated by the dashed lines. To illustrate that such payoff level alignment promotes cooperation, consider a D -action player in $V_D(3, 2)$ with two C -action neighbors. If one of these neighbors belongs to a level of higher payoffs, i.e., $V_C(2, 1)$, $V_C(3, 2)$ or $V_C(4, 3)$, and this C -action neighbor is chosen to trigger an action update, then the D -action player will switch across the band to the level $V_C(3, 2)$ with an accompanying change in the neighborhood of the reference player to place him into $V_C(2, 2)$, $V_C(3, 3)$ or $V_C(4, 4)$. These levels are of the highest payoffs in the C -band and the central site of such configurations will not be affected by the action switching mechanism. The net effect is, therefore, to promote cooperation by opening up channels for D -action players to switch to C -action and to protect the C -action players from switching back. When dilution is too high, however, isolated players and isolated pairs of players start to emerge and the effect of the term \mathcal{F}_C^I has to be included.

The qualitative picture described above can be verified numerically. From simulations, we can extract the numbers $N_C(k, n_C)$ for C -action players and $N_D(k, n_C)$ for D -action players with exactly n_C neighbors of C -action among his k neighbors after the transient. Figure 7 shows the ratios $\mathcal{F}_C^{II}(4, n_C) = N_C(4, n_C)/N$ and $\mathcal{F}_D^{II}(4, n_C) = N_D(4, n_C)/N$ as a function of n_C for the case of a full lattice (dots). The uniform $k = 4$ lattice and the initial condition lead to a peak at $n_C = 2$ for $\mathcal{F}_C^{II}(4, n_C)$ and a peak at $n_C = 3$ for $\mathcal{F}_D^{II}(4, n_C)$. For a full lattice, $\mathcal{F}_C^{II} = \sum_{n_C} \mathcal{F}_C^{II}(4, n_C)$ and its value is restricted by the drop in $\mathcal{F}_C^{II}(4, 4)$. The corresponding results for a site occupancy of $\rho = 0.7$ are shown in Figure 8. Now, k can take on values other than 4. Note that for each k , $\mathcal{F}_C^{II}(k, k)$ is the highest, resulting in the enhanced \mathcal{F}_C^{II} relative to a full lattice. This is in accordance with the qualitative picture on promoting cooperation by introducing vacancies, as discussed based on the payoff levels above. The validity of the local-configuration approximation is further established by comparing the results of $\mathcal{F}_C^{II}(k, n_C)$ with that evaluated by LCA after iterating the LCA equations to the steady state. Results for a full lattice and for $\rho = 0.7$ are in good agreement with simulation results, as shown in Figures 7 and 8 (see open circles). The success of LCA, therefore, stems from the accurate descriptions of the distribution in the local competing environment among the players.

5 Conclusions

The effects of site dilution on cooperation in an evolutionary snowdrift game on a lattice have been studied

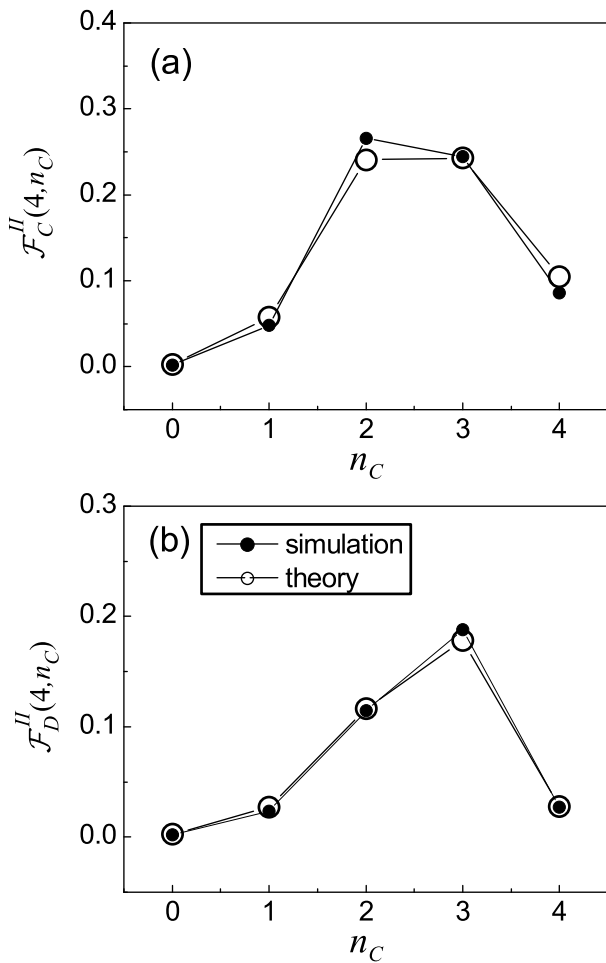


Fig. 7. The quantities (a) $\mathcal{F}_C^{II}(4, n_C)$ among sites of C -action and (b) $\mathcal{F}_D^{II}(4, n_C)$ among sites of D -action in a fully occupied square lattice, for $n_C = 0, \dots, 4$ at the cost-to-benefit ratio of $r = 0.25$ as obtained by numerical simulations (dots) and by the local-configuration approximation (open circles).

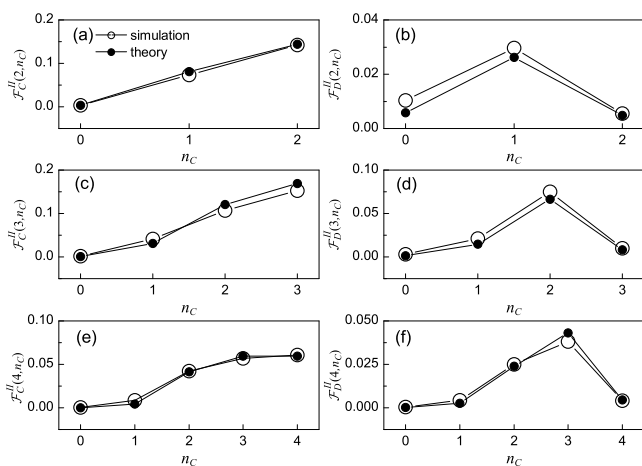


Fig. 8. The quantities (a) $\mathcal{F}_C^{II}(k, n_C)$ among sites of C -action and (b) $\mathcal{F}_D^{II}(k, n_C)$ among sites of D -action in a diluted square lattice of occupancy probability $\rho = 0.7$, for $k = 2, 3, 4$ and $n_C = 0, \dots, k$ for each value of k at the cost-to-benefit ratio of $r = 0.25$ as obtained by numerical simulations (dots) and by the local-configuration approximation (open circles).

by numerical simulations and analytic treatments. The frequency of cooperation \mathcal{F}_C generally shows a non-monotonic dependence on the fraction of occupied sites ρ , for different values of the payoff parameter r . Slightly diluting a full lattice would lead to lower cooperation for small values of r and high values of r . For a range of r , it was found dilution would lead to an enhanced cooperation. Formulating analytic approaches to evolutionary games in regular and diluted lattices is a challenging task. The importance of small clusters of players for $\rho \ll 1$ motivated us to single out their contributions to \mathcal{F}_C from the bigger clusters. The contributions \mathcal{F}_C^I from isolated players and isolated pairs of players were treated exactly. The contribution \mathcal{F}_C^{II} from the other players was first treated by the pair approximation. The results from the pair approximation do not agree with simulation results. The inadequacy of the pair approximation informs us that longer spatial correlation should be included. A local configuration approximation (LCA) was then formulated for \mathcal{F}_C^{II} . LCA treats the local competing configurations as the variables and amounts to considering a spatial extent up to the neighborhood of a player's neighbors. Results from LCA are in much better agreement with simulation results. The validity of LCA was further verified by comparing the number of different configurations extracted from simulations and obtained by LCA.

The formalism also allows for a clear physical interpretation. With a finite number of competing neighbors and thus a finite number of local configurations, the discrete payoff values for a certain action (C or D) form a set of payoff levels. Classifying these payoff levels by the number of competing neighbors k and the action (C or D) gives the notion of C -band and D -band. An initial condition amounts to distributing players into these payoff levels. When a player adapts or switches action, both his own neighborhood and the neighborhood of his competing neighbors are changed. The action-updated player makes a transition across the C -band and D -band and his neighbors make transitions within a band. The dynamics corresponds to continual re-distribution of players among the payoff levels in the bands, with the steady state properties given by the equilibrium distribution. The picture is described by the equations in LCA. The success of LCA also validates the physical picture.

We end with a few remarks. The idea behind the local configuration approximation is general and LCA can be applied to a wide range of problems. LCA can be applied to treat competing games with two actions (C or D), epidemic models with two states (susceptible or infected), and voter models with two opinions (yes or no). LCA can also be refined and applied to regular lattices as a special case [52] in problems that a reliable analytic approach is lacking, e.g. snowdrift game on lattices. LCA can be further extended to cases in which the players could take on three or more actions such as competing games incorporating a cooperative but punishing action [53] and the susceptible-infected-recovered epidemic model. Finally, the physical picture that we introduced could become a guide for formulating better theories of dynamical processes in networked entities.

This work was supported in part by the Education Department of Jiangsu Province through its Philosophy and Social Science Fund under Grant No. 2015SJD597. One of us (P.M.H.) acknowledges the support of a Direct Grant of Research in 2015 from the Faculty of Science at the Chinese University of Hong Kong.

Appendix: Pair approximation

The pair approximation amounts to studying the dynamical equations of $f_{i,j}$ and retaining spatial correlation only up to that of neighboring links by decoupling longer spatial correlations [26,48–50]. The dynamics is related to two factors - how likely a target player of current action i takes on a referencing neighbor of action j for an action update *and* how the link densities $f_{i,j}$ would be altered when such an update takes place.

To illustrate the point, first note that the probability of choosing a player I of action i who refers to a neighbor J of action j for a possible action update is $f_{i,j}$ itself. Player I has a probability $P(K-1, k_\alpha)$ of having k_α other neighbors in addition to the neighbor J . Among these k_α other neighbors, the probability of having n_C of them taking the C -action and thus $k_\alpha - n_C$ taking the D -action is $\binom{k_\alpha}{n_C} (f_{i,C}/f_i)^{n_C} (f_{i,D}/f_i)^{k_\alpha - n_C}$. Similarly for player J , he has a probability $P(K-1, k_\beta)$ of having k_β other neighbors in addition to the neighbor I . Among these k_β neighbors, the probability of having m_C of them taking the C -action and thus $k_\beta - m_C$ taking the D -action is $\binom{k_\beta}{m_C} (f_{j,C}/f_j)^{m_C} (f_{j,D}/f_j)^{k_\beta - m_C}$. Recall that the probability that player I gives up his current action and adopts player J 's action j is $w_{i \rightarrow j} = (V_{I,i} - V_{J,j})/\Omega$. Putting all the factors together, the probability of the event that the player I updates his strategy to that of his neighboring player J is given by the expression

$$P(K-1, k_\alpha) \binom{k_\alpha}{n_C} \left(\frac{f_{i,C}}{f_i}\right)^{n_C} \left(\frac{f_{i,D}}{f_i}\right)^{k_\alpha - n_C} \\ \times P(K-1, k_\beta) \binom{k_\beta}{m_C} \left(\frac{f_{j,C}}{f_j}\right)^{m_C} \left(\frac{f_{j,D}}{f_j}\right)^{k_\beta - m_C} f_{i,j} w_{i \rightarrow j}. \quad (\text{A.1})$$

Accompanying such an event of action update are changes in the link densities. Some link densities are reduced. The link densities of the types $(i-j)$ and $(j-i)$ decrease by $1/\mathcal{L}$. In addition, the link densities of the types $(i-C)$ and $(C-i)$ decrease by n_C/\mathcal{L} , and that of the types $(i-D)$ and $(D-i)$ decrease by $(k_\alpha - n_C)/\mathcal{L}$. Some link densities, however, are enhanced. The link densities of the type $(j-j)$ increases by $2/\mathcal{L}$. In addition, the link densities of the types $(j-C)$ and $(C-j)$ increase by n_C/\mathcal{L} , and that of the types $(j-D)$ and $(D-j)$ increase by $(k_\alpha - n_C)/\mathcal{L}$.

The master equations of the variables $f_{i',j'}$ can then be established by including all possible events, i.e. all values of k_α , k_β , n_C , m_C , and all possible switching from i to j .

Explicitly, we have

$$\frac{df_{i',j'}}{dt} = \frac{1}{\mathcal{L}} \sum_{i=C,D} \sum_{k_\alpha=0}^{K-1} P(K-1, k_\alpha) \\ \times \sum_{n_C}^{k_\alpha} \left(\frac{f_{i,C}}{f_i}\right)^{n_C} \left(\frac{f_{i,D}}{f_i}\right)^{k_\alpha - n_C} \\ \times \sum_{j=C,D} \sum_{k_\beta=0}^{K-1} P(K-1, k_\beta) \\ \times \sum_{m_C}^{k_\beta} \left(\frac{f_{j,C}}{f_j}\right)^{m_C} \left(\frac{f_{j,D}}{f_j}\right)^{k_\beta - m_C} f_{i,j} w_{i \rightarrow j} \\ \times [-(\delta_{i,i'} \delta_{j,j'} + \delta_{j,i'} \delta_{i,j'}) \\ - n_C (\delta_{i,i'} \delta_{C,j'} + \delta_{C,i'} \delta_{i,j'}) \\ - (k_\alpha - n_C) (\delta_{i,i'} \delta_{D,j'} + \delta_{D,i'} \delta_{i,j'}) + 2\delta_{j,i'} \delta_{j,j'} \\ + n_C (\delta_{j,i'} \delta_{C,j'} + \delta_{C,i'} \delta_{j,j'}) \\ + (k_\alpha - n_C) (\delta_{j,i'} \delta_{D,j'} + \delta_{D,i'} \delta_{j,j'})], \quad (\text{A.2})$$

where the terms with the Kronecker delta function $\delta_{i,j}$ give the change in the link density $f_{i',j'}$ when an action update occurs, and the term corresponding to $k_\alpha = 0$ and $k_\beta = 0$ is excluded from the summations over k_α and k_β . Solving the coupled equations (Eq. (A.2)) for two link densities will be sufficient. The equations can be iterated in time to convergence for obtaining the steady state behavior. Note that the occupancy probability ρ is carried in the factors $P(K-1, k)$ and the cost-to-benefit ratio r is carried in the action updating probability $w_{i \rightarrow j}$.

References

1. R. Axelrod, W.D. Hamilton, *Science* **211**, 1390 (1981)
2. R.M. May, *Nature* **292**, 291 (1981)
3. M.A. Nowak, R.M. May, *Nature* **359**, 826 (1992)
4. K. Brauchli, T. Killingback, M. Doebeli, *J. Theor. Biol.* **200**, 405 (1999)
5. G. Szabó, C. Hauert, *Phys. Rev. Lett.* **89**, 118101 (2002)
6. F.C. Santos, J.M. Pacheco, *Phys. Rev. Lett.* **95**, 098104 (2005)
7. M.A. Nowak, *Science* **314**, 1560 (2006)
8. O. Gräser, C. Xu, P.M. Hui, *New J. Phys.* **13**, 083015 (2011)
9. Z. Wang, A. Szolnoki, M. Perc, *Sci. Rep.* **2**, 369 (2012)
10. R. Axelrod, *The Evolution of Cooperation* (Basic Books, New York, 1984)
11. M. Nakamaru, H. Matsuda, Y. Iwasa, *J. Theor. Biol.* **184**, 65 (1997)
12. V.C.L. Hutson, G.T. Vickers, *Phil. Trans. R. Soc. London B* **348**, 393 (1995)
13. P. Grim, *BioSystems* **37**, 3 (1996)
14. M.A. Nowak, S. Bonhoeffer, R.M. May, *Proc. Natl. Acad. Sci. USA*, **91**, 4877 (1994)
15. F.C. Santos, J.M. Pacheco, T. Lenaerts, *Proc. Natl. Acad. Sci. USA*, **103**, 3490 (2006)
16. A. Cassar, *Games Econ. Behav.* **58**, 209 (2007)
17. L.-X. Zhong, D.-F. Zheng, B. Zheng, C. Xu, P.M. Hui, *EPL* **76**, 724 (2006)

18. V. Sasidevan, S. Sinha, *Sci. Rep.* **5**, 13071 (2015)
19. A. Bovier, *Statistical Mechanics of Disordered Systems* (Cambridge University Press, Cambridge, 2006)
20. D. Stauffer, A. Aharony, *Introduction to Percolation Theory*, 2nd edn. (Taylor & Francis, 1992)
21. J. Marro, A. Labarta, J. Tejada, *Phys. Rev. B* **34**, 347 (1986)
22. M.H. Vainstein, J.J. Arenzon, *Phys. Rev. E* **64**, 051905 (2001)
23. J.-Y. Guan, Z.-X. Wu, Y.-H. Wang, *Chin. Phys.* **16**, 3566 (2007)
24. M.A. Nowak, S. Bonhoeffer, R.M. May, *Int. J. Bifurc. Chaos* **4**, 33 (1994)
25. E.A. Sicardi, H. Fort, M.H. Vainstein, J.J. Arenzon, *J. Theor. Biol.* **256**, 240 (2009)
26. C. Hauert, M. Doebeli, *Nature* **428**, 643 (2004)
27. B. Skyrms, *The Stag Hunt and the Evolution of Social Structure* (Cambridge University Press, Cambridge, 2004)
28. W. Zhang, C. Xu, P.M. Hui, *Eur. Phys. J. B* **86**, 196 (2013)
29. M.G. Zimmermann, V.M. Eguíluz, *Phys. Rev. E* **72**, 056118 (2005)
30. O. Gräser, C. Xu, P.M. Hui, *EPL* **87**, 38003 (2009)
31. F. Vazquez, V.M. Eguíluz, M. San Miguel, *Phys. Rev. Lett.* **100**, 108702 (2008)
32. G. Demirel, F. Vazquez, G.A. Böhme, T. Gross, *Physica D* **267**, 68 (2014)
33. C.-P. Zhu, H. Kong, L. Li, Z.-M. Gu, S.-J. Xiong, *Physica A* **375**, 1378 (2011)
34. M. Ji, C. Xu, C.W. Choi, P.M. Hui, *New J. Phys.* **15**, 113024 (2013)
35. T. Gross, C. D'Lima, B. Blasius, *Phys. Rev. Lett.* **96**, 208701 (2006)
36. T. Gross, I. Kevrekidis, *EPL* **82**, 38004 (2008)
37. L.B. Shaw, I.B. Schwartz, *Phys. Rev. E* **77**, 066101 (2008)
38. O. Gräser, P.M. Hui, C. Xu, *Physica A* **390**, 906 (2011)
39. C. Nardini, B. Kozma, A. Barrat, *Phys. Rev. Lett.* **100**, 158701 (2008)
40. V. Marceau, P.-A. Noël, L. Hébert-Dufresne, A. Allard, L.J. Dubé, *Phys. Rev. E* **82**, 036116 (2010)
41. J.P. Gleeson, *Phys. Rev. Lett.* **107**, 068701 (2011)
42. P. Holme, M.E.J. Newman, *Phys. Rev. E* **74**, 056108 (2006)
43. R. Durrett, J.P. Gleeson, A.L. Lloyd, P.J. Mucha, F. Shi, D. Divakoff, J.E.S. Socolar, C. Varghese, *Proc. Natl. Acad. Sci. USA* **109**, 3682 (2012)
44. F. Vazquez, V.M. Eguíluz, *New J. Phys.* **10**, 063011 (2008)
45. P. Klimek, R. Lambiotte, S. Thurner, *EPL* **82**, 28008 (2008)
46. P. Weiss, *J. Phys.* **6**, 661 (1907)
47. P. Fulde, *Electron Correlations in Molecules and Solids* (Springer, 2002)
48. Y. Harada, Y. Iwasa, *Res. Popul. Ecol.* **36**, 237 (1994)
49. S.P. Ellner, *J. Theor. Biol.* **210**, 435 (2001)
50. F. Fu, M.A. Nowak, C. Hauert, *J. Theor. Biol.* **266**, 358 (2010)
51. Y.-C. Ni, H.P. Yin, C. Xu, P.M. Hui, *Eur. Phys. J. B* **80**, 233 (2011)
52. C. Xu, P.M. Hui, unpublished
53. N.W.H. Chan, C. Xu, S.K. Tey, Y.J. Yap, P.M. Hui, *Physica A* **392**, 168 (2013)